HHS Public Access

Author manuscript

Magn Reson Med. Author manuscript; available in PMC 2015 August 01.

Published in final edited form as:

Magn Reson Med. 2014 August ; 72(2): 485–491. doi:10.1002/mrm.24942.

Cardiac R2* values are independent on the image analysis approach employed

Antonella Meloni[1,2], **Hugh Young Rienhoff Jr**[3], **Amber Jones**[3], **Alessia Pepe**[1], **Massimo Lombardi**[1], and **John C. Wood**[2,4]

[1]CMR Unit, Fondazione G. Monasterio CNR-Regione Toscana and Institute of Clinical Physiology, Pisa, Italy.

[2]Department of Pediatrics, Division of Cardiology, Children's Hospital Los Angeles, Los Angeles, California.

[3]FerroKin BioSciences, Inc., a wholly-owned subsidiary of Shire Pharmaceuticals LLC, Wayne, Pennsylvania.

[4]Department of Radiology, Children's Hospital Los Angeles, Los Angeles, California.

Abstract

Purpose—To determine whether systematic differences were present between myocardial R2* values obtained with two different decay models: truncation and exponential-plus-constant (Exp-C).

Methods—Single-center cohorts were used to compare black and bright blood sequences separately and a multi-center cohort of mixed bright and black blood studies was used to assess the generalizability. Truncated exponential estimates were calculated with CMRTools that uses a single region of interest (ROI) method. Exp-C estimates were calculated using a pixelwise approach.

Results—No differences could be distinguished based upon whether a white or black blood sequence was examined. The two fitting algorithms gave similar R2* values, with R-squared values exceeding 0.997 and CoV of 3–4%. Results using the pixelwise method yielded a small systematic bias (~3%) that became apparent in patients with severe iron deposition. This disparity disappeared when Exp-C fitting was used on a single ROI suggesting that the use of pixelwise mapping was responsible for the bias. In the multicenter cohort the strong agreement between the two fitting approaches was reconfirmed.

Conclusion—Cardiac R2* values are independent of the signal model used for its calculation over clinically relevant ranges. Clinicians can compare results among centers using these disparate approaches with confidence.

Keywords

Cardiovascular magnetic resonance; Cardiac R2*; iron overload; image analysis

Address for correspondence: John C. Wood, Division of Cardiology, MS#34, Children's Hospital of Los Angeles, 4650 Sunset Blvd, Los Angeles, CA, 90027-0034, 323 361 5470, 323 361 7317, jwood@chla.usc.edu.

INTRODUCTION

Estimation of myocardial iron stores is essential for preventing cardiac disease and managing chelation treatment in patients with thalassemia, sickle cell disease, aplastic anemia, myelodysplasia, and other iron-related diseases (1,2). Cardiovascular magnetic resonance (CMR) is noninvasive and clinically validated for this purpose (3,4). Iron causes the darkening of gradient-echo CMR images and the rate of darkening (R2*) is proportional to the tissue iron content (5); the inverse of R2*, called T2*, is also commonly used to characterize cardiac iron burden.

The R2* value is obtained by fitting the CMR signal at different echo times (TEs) to an appropriate decay model. In heavily iron-overloaded hearts, the rapid signal loss leads to a plateau in the signal decay curve at later echo times. In this situation, fitting a simple mono-exponential model to all of the echo times produces large R2* underestimation errors (6,7). Two approaches are used to resolve this problem. The first approach (truncation model) consists of manually limiting the mono exponential equation to a few echo times. Measurements are calculated from a full-thickness septal region of interest (ROI). This approach has been implemented within different validated softwares: the CMRTools (Cardiovascular Imaging Solutions Ltd, London, UK), used firstly by the Pennell's group (7,8) and acquired by different CMR centers worldwide (9,10), the HIPPO MIOT®, used by the 8 CMR centers of the Myocardial Iron Overload in Thalassemia (MIOT) Network (11,12), and the CMR42 (Circle Cardiovascular Imaging, Canada). The second approach consists in fitting the signal with an exponential plus a constant offset. R2* values are calculated from every pixel in the interventricular septum and the median R2* is reported. It is advocated by some, including our laboratory (6), and recently has been independently implemented in an open-source software (13).

It is important for patient management that the calculated R2* values (or T2* values) are independent from the software used. Two prior reports suggested that large differences may exist (7,14). Thus we compared cardiac R2* values using the two fitting models in two disparate patient populations to determine whether systematic differences were evident.

METHODS

Study population

Two single-center cohorts and one multi-center cohort of patients were considered. The first single-center cohort included 42 patients (24 with thalassemia major, 13 with sickle cell disease, and 5 with other iron-related diseases) scanned using a black blood T2* technique. Mean age was 19.3 ± 10.1 years and 21 patients were females. The second single-center cohort included 70 patients (31 with thalassemia major, 21 with sickle cell disease, and 18 with other iron-related diseases) scanned using a white-blood T2* technique. Mean age was 18.7 ± 10.9 years and 30 patients were females. Our thalassemia cohort is 24% Chinese, 20% other Southeast Asia (Vietnamese, Laotian, Cambodian, Thai, Filipino), 17% Indian Subcontinent (Indian, Pakastani), 23% Mediterranean (Italian, Greek, Cypriot), 9% Middle Eastern (Iranian, Lebanese, Iraqi, Saudia Arabia) and 4.5% Hispanic and 2.5% other ethnic backgrounds. Our sickle cell disease cohort is 95% African descent and 5% Hispanic.

Multicenter data represented baseline measurements from a phase II clinical trial of FBS0701 (15). These data were used as a test set because they were collected according to local, clinical practice from eight major thalassemia centers. Half of the centers used white-blood acquisitions and half used black-blood techniques. Sixty-two patients of mixed race (17 Asian, 5 Black, 5 Thai and 35 White) participated with sites contributing between four and thirteen examinations (median, seven cases). Thirty patients were females and mean age was 27.9 ± 8.9 years. Fifty-eight patients suffered from thalassemias and 4 from sickle cell disease and all were regularly transfused and chelated.

The distribution of the patients is reported in Table 1.

The protocol was approved by The Children's Hospital of Los Angeles' Committee for the Protection of Human Subjects (Protocol # CCI-12-00087) and the institutional review boards of all participating hospitals. The requirement for consent was waived for the retrospective data analysis. All patients in the prospective FBS0701 trial gave written informed consent.

MRI Acquisition

Both single-center cohorts underwent CMR at the Children's Hospital of Los Angeles (CHLA), but using two different 1.5T scanners: a Philips Achieva (Philips Medical Systems, Best, The Netherlands) running system 2.5.1 and a GE Signa CVi (GE Healthcare, Waukesha, WI) running system 9.1; similar phased array torso coils were used on both. Black blood multiecho gradient echo images were used to calculate R2* on the Philips while bright blood multiecho gradient echo R2* sequence was used on the GE scanner.

For the multi-center cohort gradient echo images were acquired on 1.5T scanners from all 3 major MR vendors. Black or bright blood acquisitions were used (Figure 1).

At the CHLA as well as in all the other sites a single short axis mid-ventricular slice was acquired. All R2* sequence parameters are indicated in Table 1.

R2* measurement

All images were processed by the same operator. Identical regions of interest (ROI's) were drawn in the mid-ventricular septum for both techniques. Truncated exponential estimates were calculated using CMRTools. It calculates the mean signal intensity of the ROI for each image and fits the decay curve to a mono-exponential model:

$$S = S_0 e^{-\frac{TE}{T2^*}} \quad [1]$$

where S=fitted signal, S_0=initial amplitude, TE=echo time. The R-square value describing the goodness of fitting was used by the operator as guide in the application of the truncation model. If the R-square value was > 0.99, no truncation was applied. Otherwise, the last points were discarded in succession until the R-square value became > 0.99. Finally, the R2* value was calculated as 1000/T2*.

Exponential + constant (Exp-C) estimates were calculated using a rapid pseudo-pixelwise implementation written in MATLAB (The Mathworks, Natick, MA). This software, called Iron, divides the ROI into subregions of similar-relaxivity; the number of pixels in each subregion is equal to the square-root of the total number of pixels in the traced ROI. Each subregions is fitted to a Exp-C model:

$$S = S_0 e^{-TE \bullet R2^*} + C \quad [2]$$

where S=fitted signal, S_0=initial amplitude, TE=echo time, R2* is the relaxivity, and C is the constant offset term. A distribution of R2* values is produced and the mean and median from this distribution are obtained (16). We also implemented equation 2 over the entire ROI, similar to CMRTools, to distinguish whether differences in measured R2* values resulted from the underlying fitting model (equations 1 and 2) or from the use of a pixelwise rather than a region-based approach.

Hereafter we refer to the R2* values obtained with the CMRTools as $R2^*_{CMRTools}$ and to the R2* values obtained using Iron as $R2^*_{Iron\text{-}mean}$ (mean of R2* distribution taken into account), $R2^*_{Iron\text{-}median}$ (median of R2* distribution taken into account) and $R2^*_{Iron\_ROI\_based}$ (single ROI).

Statistical analysis

All data were analyzed using SPSS version 16.0 (SPSS Inc., Chicago, IL, USA) and MedCalc for Windows version 7.2.1.0 (MedCalc Software, Mariakerke, Belgium) statistical packages.

Continuous variables were described as mean ± standard deviation (SD).

Summary data were displayed using scatter plots with regression lines. Linear regression models provided slope and intercept estimates and the R-squared measuring the goodness of the linear fit. Because R2* values were not normally distributed, a paired Wilcoxon signed rank test was applied to detect significant differences between two datasets while the Spearman correlation coefficient was used to assess their relationship. A coefficient of variation (CoV) was calculated as the ratio of the SD of the half mean square of the differences between the repeated values, to the general mean. The Bland-Altman (BA) technique was used to plot the absolute difference (standard BA) or the percent difference (relative BA) versus the average values between two datasets. The relative Bland-Altman plot was preferred when the variability of the differences increased as the magnitude of the measurements increased. Bias was the mean of the difference between the two methods and agreement was the mean ± 1.96 SDs.

A P value < 0.05 was considered statistically significant.

RESULTS

First single-center cohort: black blood images

Figure 2a (left) shows $R2^*_{Iron\text{-}mean}$ values as a function of $R2^*_{CMRTools}$ values. The line of best fit had a slope of 1.031 ± 0.005, significantly different from 1 (P<0.0001), and an intercept of −1.176 ± 0.379 Hz. The R-squared value for the fit was 0.999. The $R2^*_{Iron\text{-}mean}$ values were not significantly different from $R2^*_{CMRTools}$ values (48.5 ± 54.7 Hz vs 48.2 ± 53.1 Hz, P=0.945). Bland-Altman analysis demonstrated no significant bias between the two techniques, with limits of agreement of 4.8 Hz (Figure 2a, right). The CoV was 3.5%.

Relationships between $R2^*_{Iron\text{-}median}$ and $R2^*_{CMRTools}$ as well between $R2^*_{Iron\text{-}ROI\_based}$ and $R2^*_{CMRTools}$ was nearly identical to results for $R2^*_{Iron\text{-}mean}$, being well described by a straight line. In both cases Bland-Altman analysis demonstrated good agreement and the CoV was less than 4.4% (Table 2a).

Second single-center cohort: bright blood images

Figure 2b (left) shows $R2^*_{Iron\text{-}mean}$ values as a function of $R2^*_{CMRTools}$ values. The line of best fit had a slope of 1.025 ± 0.005, significantly different from 1 (P<0.0001), and an intercept of −0.741 ± 0.300 Hz. The R-squared value for the fit was 0.998. The $R2^*_{Iron\text{-}mean}$ values were not significantly different from $R2^*_{CMRTools}$ values (47.6 ± 37.9 Hz vs 47.2 ± 36.9 Hz, P=0.088). Bland Altman analysis demonstrated no significant bias between the two techniques, with limits of agreement of 3.5 Hz (Figure 2b, right). a trend toward higher values using the Exp-C method The CoV was 2.7%.

The results of the comparison between $R2^*_{Iron\text{-}median}$ and $R2^*_{CMRTools}$ and between $R2^*_{Iron\text{-}ROI\_based}$ and $R2^*_{CMRTools}$ are indicated in Table 2b. In both cases a strong linear relationship was demonstrated, the Bland-Altman analysis demonstrated no significant bias and the CoV was less than 3.5%.

Multi-center cohort

Figure 2c (left) shows $R2^*_{Iron\text{-}mean}$ values as a function of $R2^*_{CMRTools}$ values. The line of best fit had a slope of 0.989 ± 0.008, not significantly different from 1 (P=0.148), and an intercept of 0.108 ± 0.372 Hz. The R-squared value for the fit was 0.997. The $R2^*_{Iron\text{-}mean}$ values were not significantly different from $R2^*_{CMRTools}$ values (43.5 ± 22.6 Hz vs 43.8 ± 22.7 Hz, P=0.250). The CoV was 2.3%. Figure 2c (right) shows the Bland-Altman plot.

The results of the comparison between $R2^*_{Iron\text{-}median}$ and $R2^*_{CMRTools}$ and between $R2^*_{Iron\text{-}ROI\_based}$ and $R2^*_{CMRTools}$ are indicated in Table 2c. In both cases a strong linear relationship was found out and the CoV was under 2.3%.

Patients with cardiac iron

As can be inferred from the both the linear regression analysis and Bland-Altman plots, the pixelwise, Exp-C analysis yields slightly higher values at larger R2*s. To better characterize that effect for an acceptable number of patients (N=45), we pooled all patients with detectable cardiac iron ($R2^*_{CMRTools} \geq 50$ Hz). Figure 3 shows the relative Bland-Altman

plots for this subgroup of patients for pixel-wise mean, pixel-wise median, and region-based application of the Exp-C model. No significant bias was detected in all three metrics. Five patients had T2* < 6 ms. In these patients, the pixelwise mean and median (Figure 3a and 3b) was 3% higher than predicted by CMR Tools but this disparity disappeared when a global ROI was used (Figure 3c).

DISCUSSION

In the last years, CMR R2* has become a widely used accurate and noninvasive technique for monitoring heart iron overload in patients with different types of hemoglobinopathies (17,18). Potential sources of variability include image acquisition parameters and image analysis methods. A number of different studies have shown that this technique is transferable between MRI scanners in different centers (12) and from different manufacturers (8,19). A number of approaches are used for calculating cardiac R2* from the source images. Within these approaches, there is generally good intra- and inter-observer reproducibility for both bright blood (20) and black blood T2* CMR (21). However, some had reported large differences in R2* results based upon a truncated exponential fit versus fitting to an exponential with a constant offset (7,14), warranting a independent, systematic comparison of the two approaches.

In all three patient cohorts, we observed that the two fitting approaches yield similar R2* values with R-squared values exceeding 0.997, regardless of whether white or black blood images were used. More importantly, the CoV was extremely low, suggesting excellent stability of both techniques. Nonetheless, the regression slopes were ~3% greater than unity and these differences became more apparent in patients with severe iron deposition (R2* > 100 Hz). This is in agreement with two previous studies involving the liver. Beaumont et al. showed that in the liver the models differences became evident for R2* values higher than 200 Hz (22). Meloni et al. demonstrated that the relationship between hepatic $R2^*_{\text{Iron-median}}$ and $R2^*_{\text{CMRTools}}$ values was well described by a line and that results were unbiased for R2*<300 Hz, but large systematic differences in R2* appeared at higher values, with the exponential-plus-constant fits averaging ~20% higher (23). The biases arise from two sources, use of pixel-wise mapping rather than a region-based technique as well as the underlying relaxation model (Equations 1 and 2). Figure 3c suggests that it is the use of pixelwise mapping that is responsible for 3% bias, rather than the fitting model. When there is high spatial variability of tissue iron distribution, pixelwise mapping more closely reflects the true average tissue iron concentration than using a global ROI. Ghugre et al. (6) also demonstrated that, using identical signal decay models, pixelwise fits yielded 3–5% higher R2* values than a global ROI at high iron concentrations. Regardless of which approach more closely approximates true iron concentration, the systematic R2* bias between these approaches is so small that it is clinically irrelevant.

We used three different cohorts to probe the differences over as a broad a patient base as possible. We could distinguish no differences based upon whether a white or black blood sequence was examined. To obtain higher generalizability, we also included a multi-center cohort of patients scanned according to the specific protocol of their center using a mixture of white and black blood techniques. We reconfirmed the strong agreement between R2*

values obtained with the two softwares (Figure 2c). While the study was somewhat hampered by small number of patients having cardiac iron in any single cohort, the pooled sample size (N=45) was large enough to detect any significant systematic deviation. Our study might have been able to detect larger differences if our study populations included more patients with cardiac T2* < 5 ms, but such patients are becoming rare at institutions performing routine cardiac screening because diagnosis triggers intensified therapy and they tend to present with heart failure or death at centers lacking MRI screening. Since the therapy of any patient whose T2* is < 5 ms should be maximally escalated, our current data completely spans the clinically-relevant range. Furthermore our data from liver suggest the maximum error is < 15% and is detectable only when T2* falls below 3 ms (23). We cannot explain why we were unable to replicate the findings of He et al (7), however the lack of systematic bias explains why our initial in-vitro calibration curve (4) agrees closely with more recent data analyzed using CMRTools (18).

In conclusion, we showed that the cardiac R2* values are independent of the signal model (Equation 1 or 2) used for its calculation. Software using a pixel-wise approach will yield R2* values approximately 3% greater than for a region-base approach in severely iron overloaded subjects, similar to prior simulations (6). The overall variability among these techniques is exceeding small and negligible clinically. Thus, it is not likely to significantly affect clinical management or indeed lead to inappropriate management of patients. Moreover, clinicians can compare results with confidence among centers using these disparate approaches.

ACKNOWLEDGMENTS

This work was supported by a grant from the National Institutes of Health, National Heart Lung and Blood Institute (1 RO1 HL075592-01A1), the Center for Disease Control (1 U01 DD000309-1), the National Center for Research Resources, Children's Hospital Los Angeles General Clinical Research Center (RR00043-43) and FerroKin BioSciences as sponsor of the study.

We thank all patients for their cooperation.

REFERENCES

1. Wood JC, Enriquez C, Ghugre N, Otto-Duessel M, Aguilar M, Nelson MD, Moats R, Coates TD. Physiology and pathophysiology of iron cardiomyopathy in thalassemia. Ann N Y Acad Sci. 2005; 1054:386–395. [PubMed: 16339687]
2. Pepe A, Meloni A, Capra M, Cianciulli P, Prossomariti L, Malaventura C, Putti MC, Lippi A, Romeo MA, Bisconte MG, Filosa A, Caruso V, Quarta A, Pitrolo L, Missere M, Midiri M, Rossi G, Positano V, Lombardi M, Maggio A. Deferasirox, deferiprone and desferrioxamine treatment in thalassemia major patients: cardiac iron and function comparison determined by quantitative magnetic resonance imaging. Haematologica. 2011; 96(1):41–47. [PubMed: 20884710]
3. Anderson LJ, Holden S, Davis B, Prescott E, Charrier CC, Bunce NH, Firmin DN, Wonke B, Porter J, Walker JM, Pennell DJ. Cardiovascular T2-star (T2*) magnetic resonance for the early diagnosis of myocardial iron overload. Eur Heart J. 2001; 22(23):2171–2179. [PubMed: 11913479]
4. Ghugre NR, Enriquez CM, Gonzalez I, Nelson MD Jr, Coates TD, Wood JC. MRI detects myocardial iron in the human heart. Magn Reson Med. 2006; 56(3):681–686. [PubMed: 16888797]
5. Ghugre NR, Coates TD, Nelson MD, Wood JC. Mechanisms of tissue-iron relaxivity: nuclear magnetic resonance studies of human liver biopsy specimens. Magn Reson Med. 2005; 54(5):1185–1193. [PubMed: 16215963]

6. Ghugre NR, Enriquez CM, Coates TD, Nelson MD Jr, Wood JC. Improved R2* measurements in myocardial iron overload. J Magn Reson Imaging. 2006; 23(1):9–16. [PubMed: 16329085]
7. He T, Gatehouse PD, Smith GC, Mohiaddin RH, Pennell DJ, Firmin DN. Myocardial T2* measurements in iron-overloaded thalassemia: An in vivo study to investigate optimal methods of quantification. Magn Reson Med. 2008; 60(5):1082–1089. [PubMed: 18956471]
8. Tanner MA, He T, Westwood MA, Firmin DN, Pennell DJ. Multi-center validation of the transferability of the magnetic resonance T2* technique for the quantification of tissue iron. Haematologica. 2006; 91(10):1388–1391. [PubMed: 17018390]
9. Au WY, Lam WW, Chu W, Tam S, Wong WK, Liang R, Ha SY. A T2* magnetic resonance imaging study of pancreatic iron overload in thalassemia major. Haematologica. 2008; 93(1):116–119. [PubMed: 18166794]
10. Bayraktaroglu S, Aydinok Y, Yildiz D, Uluer H, Savas R, Alper H. The relationship between the myocardial T2* value and left ventricular volumetric and functional parameters in thalassemia major patients. Diagn Interv Radiol. 2011; 17(4):346–351. [PubMed: 21647857]
11. Meloni A, Ramazzotti A, Positano V, Salvatori C, Mangione M, Marcheschi P, Favilli B, De Marchi D, Prato S, Pepe A, Sallustio G, Centra M, Santarelli MF, Lombardi M, Landini L. Evaluation of a web-based network for reproducible T2* MRI assessment of iron overload in thalassemia. Int J Med Inform. 2009; 78(8):503–512. [PubMed: 19345609]
12. Ramazzotti A, Pepe A, Positano V, Rossi G, De Marchi D, Brizi MG, Luciani A, Midiri M, Sallustio G, Valeri G, Caruso V, Centra M, Cianciulli P, De Sanctis V, Maggio A, Lombardi M. Multicenter validation of the magnetic resonance t2* technique for segmental and global quantification of myocardial iron. J Magn Reson Imaging. 2009; 30(1):62–68. [PubMed: 19557847]
13. Messroghli DR, Rudolph A, Abdel-Aty H, Wassmuth R, Kuhne T, Dietz R, Schulz-Menger J. An open-source software tool for the generation of relaxation time maps in magnetic resonance imaging. BMC Med Imaging. 2010; 10:16. [PubMed: 20673350]
14. He T, Gatehouse PD, Kirk P, Mohiaddin RH, Pennell DJ, Firmin DN. Myocardial T*2 measurement in iron-overloaded thalassemia: an ex vivo study to investigate optimal methods of quantification. Magn Reson Med. 2008; 60(2):350–356. [PubMed: 18666131]
15. Neufeld EJ, Galanello R, Viprakasit V, Aydinok Y, Piga A, Harmatz P, Forni GL, Shah FT, Grace RF, Porter JB, Wood JC, Peppe J, Jones A, Rienhoff HY Jr. A phase 2 study of the safety, tolerability, and pharmacodynamics of FBS0701, a novel oral iron chelator, in transfusional iron overload. Blood. 2012; 119(14):3263–3268. [PubMed: 22251482]
16. Saiviroonporn P, Viprakasit V, Boonyasirinant T, Khuhapinant A, Wood JC, Krittayaphong R. Comparison of the region-based and pixel-wise methods for cardiac T2* analysis in 50 transfusion-dependent Thai thalassemia patients. J Comput Assist Tomogr. 2011; 35(3):375–381. [PubMed: 21586934]
17. Wood JC, Tyszka JM, Carson S, Nelson MD, Coates TD. Myocardial iron loading in transfusion-dependent thalassemia and sickle cell disease. Blood. 2004; 103(5):1934–1936. [PubMed: 14630822]
18. Carpenter JP, He T, Kirk P, Roughton M, Anderson LJ, de Noronha SV, Sheppard MN, Porter JB, Walker JM, Wood JC, Galanello R, Forni G, Catani G, Matta G, Fucharoen S, Fleming A, House MJ, Black G, Firmin DN, St Pierre TG, Pennell DJ. On T2* magnetic resonance and cardiac iron. Circulation. 2011; 123(14):1519–1528. [PubMed: 21444881]
19. Westwood MA, Firmin DN, Gildo M, Renzo G, Stathis G, Markissia K, Vasili B, Pennell DJ. Intercentre reproducibility of magnetic resonance T2* measurements of myocardial iron in thalassaemia. Int J Cardiovasc Imaging. 2005; 21(5):531–538. [PubMed: 16175443]
20. Pepe A, Positano V, Santarelli F, Sorrentino F, Cracolici E, De Marchi D, Maggio A, Midiri M, Landini L, Lombardi M. Multislice multiecho T2* cardiovascular magnetic resonance for detection of the heterogeneous distribution of myocardial iron overload. J Magn Reson Imaging. 2006; 23(5):662–668. [PubMed: 16568436]
21. Smith GC, Carpenter JP, He T, Alam MH, Firmin DN, Pennell DJ. Value of black blood T2* cardiovascular magnetic resonance. J Cardiovasc Magn Reson. 2011; 13:21. [PubMed: 21401929]

22. Beaumont M, Odame I, Babyn PS, Vidarsson L, Kirby-Allen M, Cheng HL. Accurate liver T2 measurement of iron overload: a simulations investigation and in vivo study. J Magn Reson Imaging. 2009; 30(2):313–320. [PubMed: 19629985]

23. Meloni A, Rienhoff HY Jr, Jones A, Pepe A, Lombardi M, Wood JC. The use of appropriate calibration curves corrects for systematic differences in liver R2* values measured using different software packages. Br J Haematol. 2013; 161(6):888–891. [PubMed: 23496418]

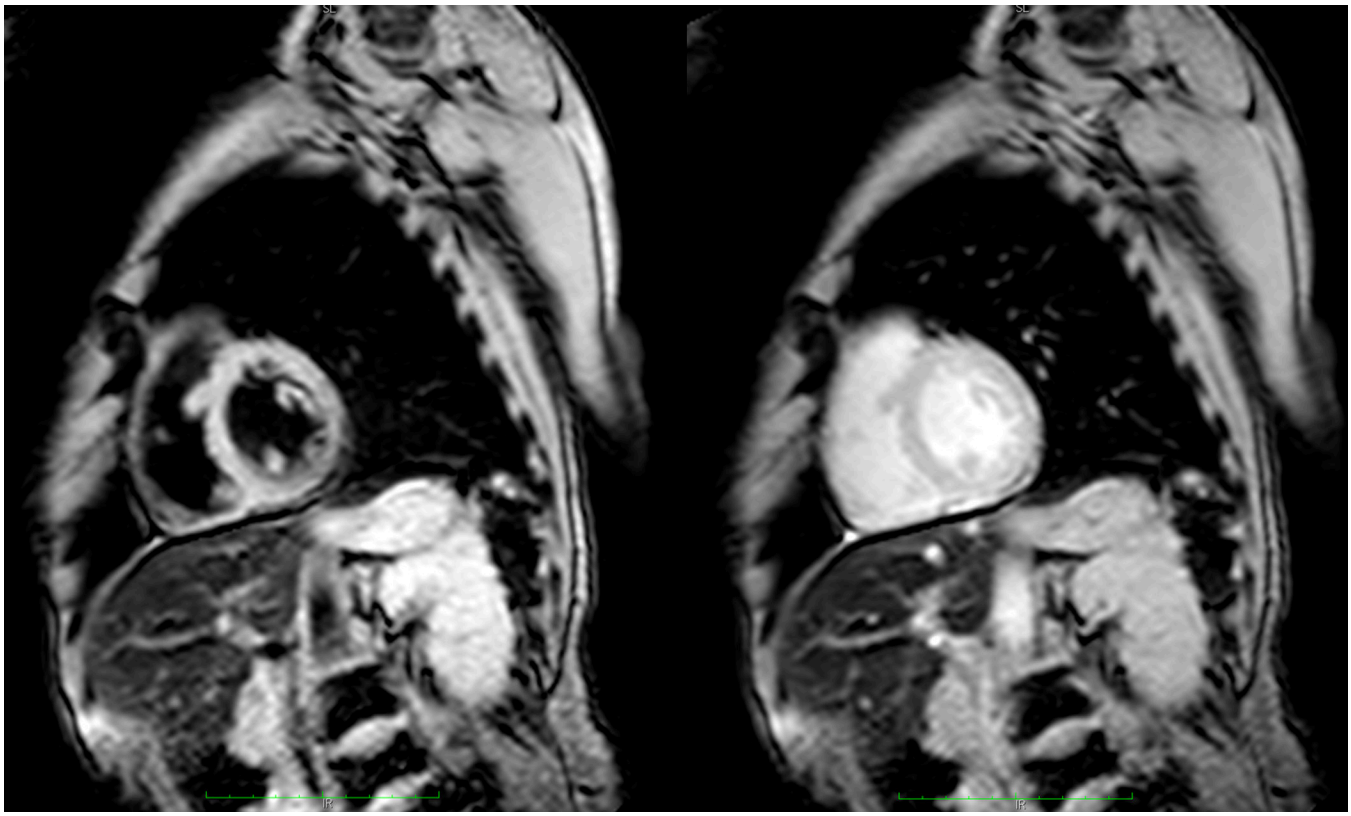

Figure 1.
Typical black blood (left) and bright blood (right) short-axis mid-ventricular images at the first echo time.

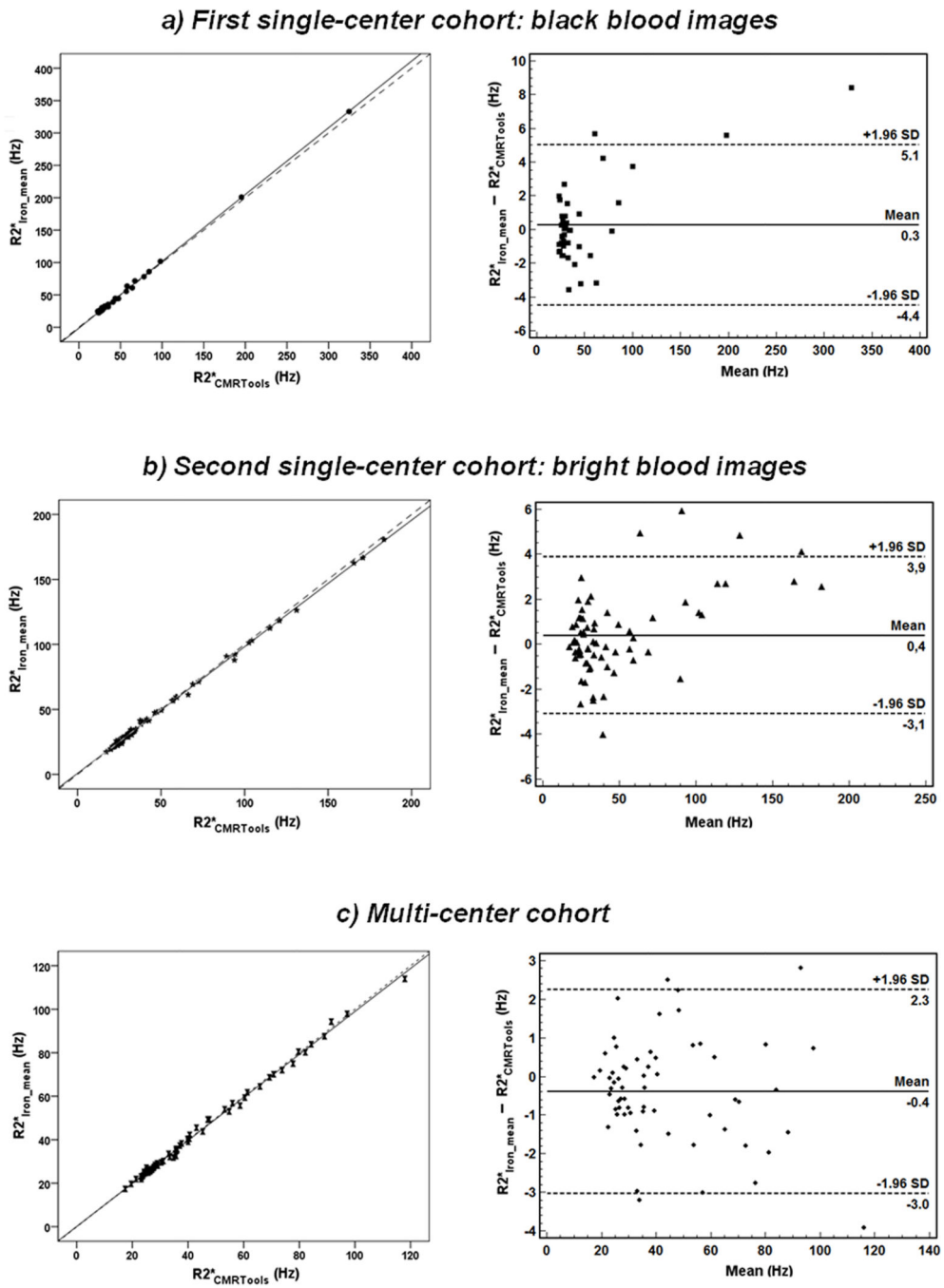

Figure 2.

Comparison between $R2^*_{Iron\text{-}mean}$ values and $R2^*_{CMRTools}$ values for a) the first single-center cohort (black blood images), b) the second single-center cohort (bright blood images) and c) the multi-center cohort. Left: Scatter plot with regression line (solid line). The dotted line is the line of identity. Right: Bland-Altman plot of absolute differences. Dotted lines indicate the limits of agreement.

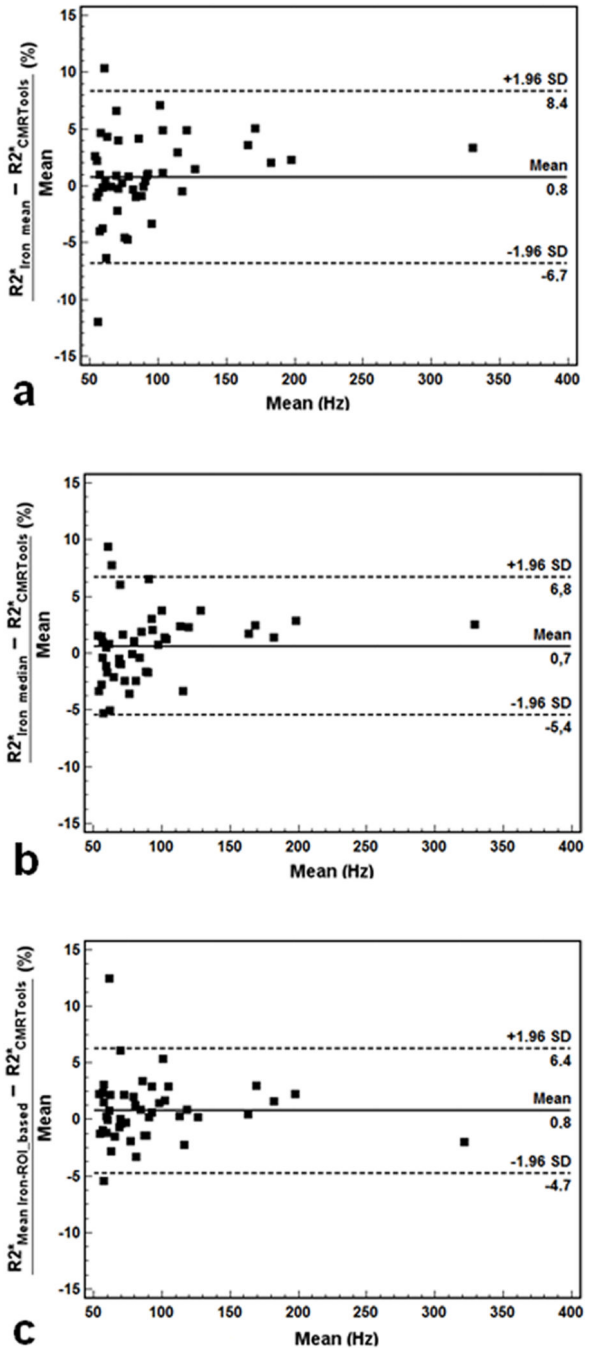

Figure 3.

Agreement between the two methods for all patients with detectable cardiac iron. Relative Bland-Altman plots for a) $R2^*_{Iron\text{-}mean}$ and $R2^*_{CMRTools}$ values, b) $R2^*_{Iron\text{-}median}$ and $R2^*_{CMRTools}$ values and c) $R2^*_{Iron\text{-}ROI\_based}$ and $R2^*_{CMRTools}$ values.

Table 1

R2* sequence parameters for all the sites involved in this study.

	Single center		Multi center						
	Los Angeles, USA		Boston, USA	Cagliari, Italy	Genoa, Italy	Izmir, Turkey	London, UK	Oakland, USA	Siriraj, Thailand
# patients	42	70	4	15	6	11	6	7	13
Scanner	Philips Achieva	GE Signa	Philips	Siemens	GE LX	Siemens Symphony	Siemens Avanto	Philips Achieva	Philips Achieva
Field strength (Tesla)	1.5	1.5	1.5	1.5	1.5	1.5	1.5	1.5	1.5
Software release	2.6.3.5	9.1	2.6.3.5	VB15	15.0 M4 0910.a	VA30A	VB17	2.6.3	2.6.3.5
Coil	body	torso	4-channel torso	8-channel cardiac	8-channel cardiac	Phased-array body	4-channel torso	Phased array body	5-channel cardiac
Sequence	Black blood	Bright blood	Black blood	Bright Blood	Bright blood	Bright blood	Bright blood	Black blood	Black blood
Min TE (ms)	1.28	1.46	2	2.59	1.4	2.6	2.59	1.92	2
ΔTE (ms)	1.09	2.38	2.14	2.23	1	2.69	2.23	2.01	2.02
# echoes	16	8	8	8	8	8	8	8	8
FA (°)	20	20	20	20	20	20	20	20	20
Matrix (pixels)	256 × 256	256 × 256	128 × 128	128 × 256	128 × 96	192 × 75	256 × 96	125 × 156	128 × 256
Field of view (cm)	30–36	30–36	25–32	35–40	31–40	40	40	23–36	40
Bandwith (Hz/pixel)	1563	488	723	810	648	810	810	720	382
Slice thk (mm)	8	8	8	10	8	10	10	8	10

Table 2

$R2^*_{Iron\text{-}median}$ and $R2^*_{Iron\text{-}ROI\_based}$ versus $R2^*_{CMRTools}$ for the three cohorts of patients.

	Paired t-test		Regression Analysis				Bland Altman		CoV (%)
	Mean Values (Hz)	P	Slope	P for Slope ≠1	Intercept (Hz)	R-squared	Mean diff (Hz)	Limits (Hz)	
a) First single-center cohort: black blood images									
$R2^*_{Iron\text{-}median}$ vs $R2^*_{CMRTools}$	48.9±55.0 vs 48.2±53.1	0.258	1.036±0.007	<0.0001	−1.007±0.473	0.998	0.7	−5.0 to 6.5	4.37
$R2^*_{Iron\text{-}ROI\_based}$ vs $R2^*_{CMRTools}$	48.9±52.7 vs 48.2±53.1	0.063	0.993±0.007	0.336	1.058± 0.512	0.998	0.7	−4.1 to 5.5	3.66
b) Second single-center cohort: bright blood images									
$R2^*_{Iron\text{-}median}$ vs $R2^*_{CMRTools}$	47.7±38.2 vs 47.2±36.9	0.085	1.035±.006	<0.0001	−1.190±0.373	0.998	0.4	−4.0 to 4.9	3.45
$R2^*_{Iron\text{-}ROI\_based}$ vs $R2^*_{CMRTools}$	47.5±37.4 vs 47.2±36.9	0.050	1.013±0.004	0.002	−0.245±0.247	0.999	0.4	−2.3 to 3.0	2.06
c) Multi-center cohort									
$R2^*_{Iron\text{-}median}$ vs $R2^*_{CMRTools}$	43.7±22.4 vs 43.8±22.7	0.989	0.982±0.007	0.015	0.705±0.359	0.997	−0.1	−2.7 to 2.6	2.25
$R2^*_{Iron\text{-}ROI\_based}$ vs $R2^*_{CMRTools}$	44.0±22.5 vs 43.8±22.7	0.207	0.989±0.007	0.131	0.681±0.352	0.997	0.2	−2.3 to 2.7	2.07